Capsaicin Activation of the Pain Receptor, VR1: Multiple Open States from Both Partial and Full Binding

Kwokyin Hui, Beiying Liu, and Feng Qin
Department of Physiology and Biophysical Sciences, State University of New York at Buffalo, Buffalo, New York 14214

ABSTRACT Capsaicin, the pungent ingredient of hot peppers, has long been used to identify nociceptors. Its molecular target, the vanilloid receptor VR1, was recently cloned and confirmed functionally as a polymodal detector of multiple pain stimuli: heat, acid, and vanilloids. Previous electrophysiology studies have focused on whole-cell characteristics of the receptor. Here, we provide the first in-depth single-channel kinetic study of VR1 to understand its activation mechanism. At low to medium concentrations, channel activity appeared as bursts. Not only did the durations of the interburst gaps vary with capsaicin, the bursts also appeared ligand-dependent, with high capsaicin prolonging bursts and stabilizing openings. Gating involved at least five closed and three open states, with strong correlations between short closures and long openings, and long closures and short openings. Increasing capsaicin reduced the long closures with little effect on short ones. The open time constants changed little with capsaicin concentration, though their relative proportions varied. These results suggest that 1), the channel contains multiple capsaicin binding sites; 2), both partial and full binding are capable of opening the channel; 3), when activated, multiple open states are accessible irrespective of the level of binding; and 4), capsaicin association occurs preferentially to the closed channel.

INTRODUCTION

Heat, acid, and ''hot'' foods stimulate a class of neurons called nociceptors which leads to the sensation of pain. Although these stimuli appear diverse in nature, a single molecule expressed in these pain-sensing neurons responds to them all (Caterina et al., 1997; Tominaga et al., 1998; Hayes et al., 2000). This molecular target, a vanilloid receptor (VR1), is a cation channel capable of responding to multiple stimuli, suggesting its unique role in integrating pain sensations. In response to heat, low pH, or capsaicin (the pungent ingredient in ''hot'' foods), calcium flows from the extracellular lumen into the cytoplasm through the channel, thereby initiating a cascade of events which leads to the sensation of pain (Szallasi and Blumberg, 1999; Caterina and Julius, 2001; Julius and Basbaum, 2001).

The cloning of VR1 in conjunction with mutagenesis studies has enlightened our views on the molecular determinants of pain sensation. Sequence analysis and biochemical studies suggest this channel is similar to that responsible for the transient-receptor potential, and to voltage and cyclic-nucleotide gated channels (Caterina et al., 1997; Rosenbaum et al., 2002; Kedei et al., 2001; Clapham et al., 2001). In comparison to these channels, the primary sequence of VR1 predicts six transmembrane helices. Neutralizations of acidic residues in the putative P-loop affect the ion selectivity and gating by capsaicin and protons, suggesting that this region is part of the extracellular pore (Garcia-Martinez et al., 2000; Welch et al., 2000; Jordt et al., 2000). Furthermore, biochemical assays on VR1 and a mixture of VR1 with a dominant-negative mutant support a tetrameric structure, which is common to these other channels (Kuzhikandathil et al., 2001; Kedei et al., 2001; Rosenbaum et al., 2002). These results suggest that VR1 may belong to the super-family of channels with six transmembrane domains.

More recently, mutagenesis studies have begun to identify molecular regions and residues involved in the ligand-dependent activation of VR1. Although capsaicin is an exogenous activator of the channel, this lipophilic compound appears to traverse the plasma membrane to reach an intracellular/intramembrane binding site (Jung et al., 1999). Chimeric studies between the capsaicin-responsive rat VR1 and the capsaicin-insensitive chick VR1 or rat VRL1 have localized a region around TM3 that might be involved in capsaicin binding (Jordt and Julius, 2002). Substitution of this region from rat VR1 into homologous regions in the other two channels conferred capsaicin-dependent activity. However, binding alone is insufficient in activating the channel. Mutation of three residues in TM6 (NML676FAP) abolished capsaicin activation with little effect on ligand binding (Kuzhikandathil et al., 2001). This uncoupling of capsaicin binding and channel activation suggests a complex allosteric gating mechanism that involves at least TM3 and TM6.

To elucidate the gating mechanism of VR1, we have examined its activation by capsaicin at the single-channel level. Most studies on the channel have been conducted at the whole-cell level, revealing general features of the wild-type protein. It is our hope that the analysis of single-channel activity can lead to a greater understanding of the molecular mechanisms of channel gating, which would be otherwise difficult to obtain from macroscopic measurements. The questions we address through these studies are: How many

Submitted September 13, 2002, and accepted for publication December 20, 2002.

Address reprint requests to Dr. Feng Qin, 124 Sherman Hall, SUNY at Buffalo, Buffalo, NY 14214. Tel.: 716-829-2764; Fax: 716-829-2569; E-mail: qin@acsu.buffalo.edu.

0006-3495/03/05/2957/12 $2.00

representative conformational states are involved in gating? How many binding steps are necessary for full activation? Is the open state of the channel unique or are there multiple pathways leading to openings? Can the channel open with only partial binding of capsaicin, or does it have to wait until all binding sites are filled? How are the different conformational states linked in the kinetic scheme of gating? Answers to these questions are essential to a greater understanding of the structure and function of the receptor.

Our goal is to establish a simple kinetic model which best approximates the experimental results of VR1 at the single-channel level. In principle, one might expect to derive such a model by evaluating all schemes. Unfortunately, the strategy rarely works in practice. First, there are an astronomical number of models making an exhaustive search impractical. Second, single-channel activity, particularly VR1, often exhibits inhomogeneous variations among channels. Blind modeling does not observe such variations and may lead to false assertions, whereas selective modeling ignores these possibly authentic fluctuations. To minimize these problems, we have adopted a two-stage approach. First, we focus on model-independent properties of the channel. The validity of the results obtained in this stage is not model-specific. With these results in hand, we can then move to the detailed modeling of the channel to establish a reasonable gating scheme. The results accumulated from the first stage can be used to limit the candidate models we need to examine.

In this article, we present the results from our model-independent studies. We describe the burst behavior and capsaicin-dependent activation of the channel in detail. We investigate the dwell-time distributions and correlations between different open and closed conformations. We explore the possible implications of our observations on the underlying gating mechanism. Our results indicate that the channel has at least five to seven closed and three to five open conformational states. Capsaicin association appears to occur preferentially to the closed channel. Both partial and full binding are capable of opening the channel, and once the channel is activated, multiple open states are accessible irrespective of the level of binding. From these findings we present a plausible model that captures all aspects of our observations.

METHODS

Oocytes expression

VR1 from rat dorsal root ganglion cloned in pFROG (generously provided by Dr. David Julius; see also Jordt et al., 2000; Caterina et al., 1997), was linearized by MluI digest. Capped mRNA was transcribed from the T7 promoter with the mMessage mMachine kit (Ambion, Austin, TX), resuspended in RNase free water to ~1 ng/nl, and kept at −80°C until use. *Xenopus* oocytes were surgically removed and stored at 15°C in Ringer's solution until use. Oocytes were defolliculated with collagenase before injection. 18–27 ng RNA was injected into each oocyte and incubated in Ringer's solution at 15°C. Oocytes were patched 2–8 days after, which gave a high success rate of acquiring single channels.

Electrophysiology

Patch pipettes were pulled from borosilicate glass (Sutter Instrument, Novato, CA) to a resistance of 6–10 MΩ. Bath and pipette solutions contained, in mM, 110 Na, 100 gluconate, 10 Cl, 10 HEPES, 5 EGTA, pH7.4 (NaOH). HEPES was purchased from Fisher (Fair Lawn, NJ), the others from Sigma (St. Louis, MO). Capsaicin (Sigma, St. Louis, MO) and capsazepine (Precision Biochemicals, Vancouver, BC, Canada) were dissolved to a concentration of 0.1–10 μM and 10 μM, respectively, in the above recording solution from a 1 mM ethanol-dissolved stock (0.001–0.1% final ethanol). Experiments were conducted at room temperature (20–25°C). Outside-out patches were formed from VR1-injected oocytes. The number of channels was determined by application of high capsaicin (>1 μM) and blocked with capsazepine, and their orientation by the conductance and the characteristic outward-rectification of the current as shown in Fig. 1 *C* (Caterina et al., 1997; Piper et al., 1999). Only single channels were used in this study. Generally, experiments were conducted starting with application of low ligand to avoid potential contamination in subsequent perfusions. Data was acquired on an Axopatch 200B amplifier (Axon Instruments, Foster City, CA) low-pass filtered at 10 kHz, digitized at 25 kHz through a BNC-2090/MIO acquisition system (National Instruments, Austin, TX), and recorded with custom-designed software using Labview 5.1 (National Instruments, Austin, TX). Because capsaicin may take some time to perfuse to equilibrium, the initial segment comprising little or no activity after application was ignored.

Burst detection

Bursts of openings were identified using a fixed closed criterion, $\tau_{crit} = 100$ ms, with little open activity ($P_o < 0.01\%$). From the closed dwell-time distributions, this value was sufficient in distinguishing between the longest closures (interburst gaps) from the others at concentrations below 1 μM (Fig. 3 *B*). At higher capsaicin levels, such long closures disappeared, and the identification of gaps often became impossible. Therefore, we limited our analysis up to 1 μM. To ensure that our burst analyses were not biased by using a fixed burst detection criterion across concentrations, we also analyzed five experiments with a critical gap duration $\tau_{crit} = 200$ ms as well as a variable τ_{crit} (Colquhoun and Hawkes, 1982). Although the absolute values of the durations were affected by the cutoff used, the concentration dependences were preserved.

Data idealization

Single-channel currents were idealized using the segmental k-means (SKM) approach based on hidden Markov modeling (Rabiner et al., 1986). Briefly, the method models the data as a discrete Markov chain embedded in white background noise. Initial model parameters, including current amplitudes, noise variances, and Markovian transition probabilities, were reasonably estimated from selected data. The Viterbi algorithm (Forney, 1973) was then applied to obtain a most likely dwell-time sequence. From the resultant idealization, the model parameters were refined, where the current amplitudes and noise variances were calculated as the standard means and variances of the samples detected for the corresponding conductance levels, and the transition probabilities were determined based on empirical counting of the occurrences of the transitions in the idealized sequence. The re-estimated parameters were then used for another iteration of idealization through the Viterbi algorithm, and the procedure was repeated until the likelihood reached its maximum. Upon convergence, the mean lifetimes and occupancy probabilities of the channel were calculated. An amplitude probability density was then constructed from the amplitude and noise variance estimates, and was superimposed with the all-points amplitude

histograms for validation of the results. The idealized dwell-time sequence was also carefully compared with the raw data for assessment of the detection accuracy (Fig. 3 *A*). In contrast to the half-amplitude threshold detection, the SKM approach takes noise into explicit account, thereby allowing for a larger background noise and a higher bandwidth. This in turn allows for a more reliable detection of the rapid opening and closing events that constitute a large portion of VR1 activity (Figs. 1 *A* and 3 *B*). Although the approach initially requires a kinetic model, the results were generally insensitive to the details of the model, presumably because the likelihood is dominated by amplitudes. Normally, a model with two closed and one open states was sufficient for satisfactory idealization.

Dwell-time histogram analysis

Both one- and two-dimensional dwell-time histograms were constructed with a fixed dead-time 40 μs, to account for instrument resolution. Dwell-times with durations shorter than the critical dead-time were removed by merging them with the adjacent ones. The dwell-time histograms were used mainly for the purpose of visual inspection of the results; the fitting was actually performed over the dwell-time sequence directly through the use of specific models, as explained below. Compared to standard exponential fitting, this permits the use of full maximum likelihood approaches without binning the data and gives the true likelihood values, which can be used as a sensitive measure for the goodness of the fit.

For analysis of one-dimensional histograms, a star model was chosen for maximum likelihood fitting. For example, to fit the closed distribution with four exponential components, a four-closed/one-open star model was employed:

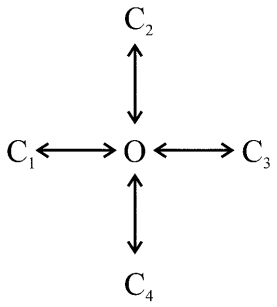

Maximum likelihood fitting of the model is equivalent to fitting the closed histogram with a linear combination of four exponentials. Fitting of an open histogram was essentially the same, except reversing the closed and open states. Other types of models can also be used, but the star model has the simplicity for easy determination of the time constants and areas (proportions) of the individual components, where the *i*th time constant is simply the reciprocal of the rate constant leaving the *i*th closed state, and the corresponding area is proportional to the reverse rate normalized to the total sum of the rates leaving the center state (*O*, in the above example). The number of components was determined by repeatedly fitting with an increasing number of surrounding states until the likelihood stopped increasing significantly. The probability density function was evaluated from the model and compared to the histograms to visually assess the accuracy of the fit.

The two-dimensional dwell-time distributions were analyzed to explore the possible existence of components not revealed by the one-dimensional histograms. Analysis of these distributions was based on the use of uncoupled, fully connected models; e.g.:

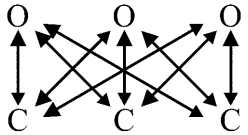

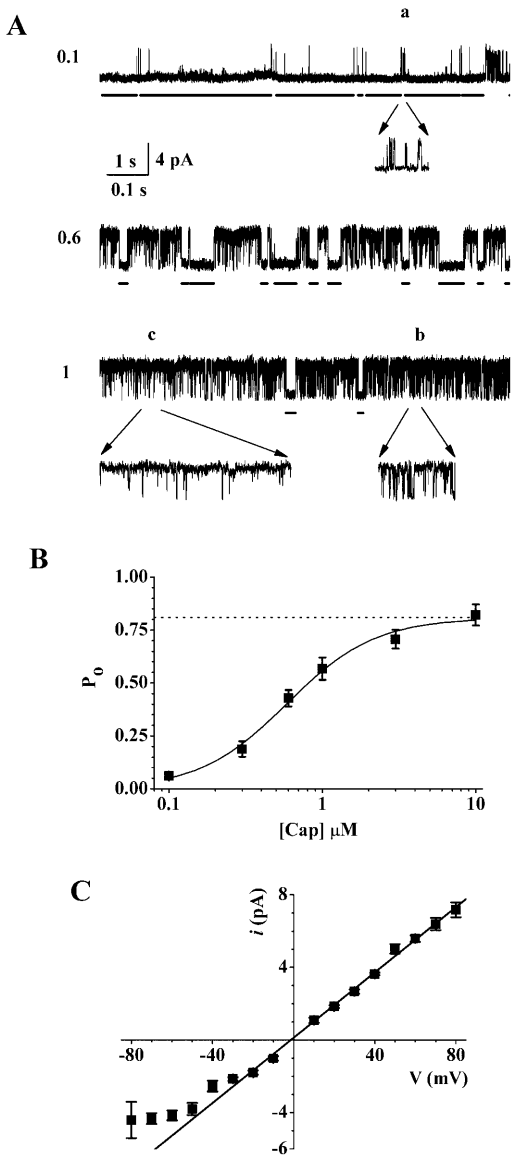

FIGURE 1 Capsaicin-activated single-channel activity from a single VR1-containing outside-out patch. (*A*) Bars below traces indicate detected gaps with the 100-ms criteria as described in the text. Three common types of burst activities are labeled above the traces and shown below on an expanded time scale: (*a*) short spiky openings with intermediate closures; (*b*) short/intermediate openings with spiky closures; and (*c*) long openings with spiky closures. Activity was elicited by the indicated ligand concentration at +60 mV. Traces were filtered at 1 kHz. (*B*) Single-channel dose-response of VR1 by capsaicin. The average open probability follows a dose-response with $n_H = 1.5 \pm 0.4$, $K_d = 0.59 \pm 0.10$ μM, and maximal $P_o = 0.81 \pm 0.04$ (*dotted line*). Each point describes mean ± SE from 16 experiments. (*C*) Unitary current-voltage relationship of VR1 by capsaicin, showing the characteristic outward rectification of the channel. The line is a best linear fit of the current at applied positive voltages. Data were averaged from 40 experiments.

A model of this topology is assured to be identifiable, and given N_c-closed and N_o-open states, it has a total of $2N_cN_o$ free parameters, which is as many as the two-dimensional dwell-time distributions can identify (Fredkin et al., 1985; Magleby and Weiss, 1990). Fitting the dwell-time sequence with this type of model is therefore equivalent to fitting two-dimensional histograms with sums of two-dimensional exponentials while maintaining the marginal

and total probability constraints (Rothberg and Magleby, 1998). The model was initially constructed based on the results of the one-dimensional fit. Additional closed and open states were then introduced to determine whether the likelihood could be improved. As in the one-dimensional case, the process was repeated until the likelihood was fully maximized.

Correlations between specific openings and closings were also explored qualitatively using two types of pseudo two-dimensional histograms. Unlike the full two-dimensional histograms, these pseudo distributions do not require a large number of events. The first type shows the dependence of the mean open duration on adjacent closed dwell-times (Kerry et al., 1988; McManus and Magleby, 1989). Here, the closed dwell-times are divided into as many bins as in the one-dimensional histogram, but the open times are simply lumped together to give an average. The second type is similar to the full two-dimensional histogram, but with less numbers of bins. Here, the distributions of openings adjacent to three types of closures, representing brief flickers (short), events of intermediate duration (medium), and gaps (long), are plotted. This latter distribution is similar to taking slices at different closed dwell-times from the full two-dimensional histogram.

Estimating rate constants

The rate constants for a given gating scheme were determined using a maximum interval likelihood approach (Qin et al., 1996, 1997). Briefly, the method evaluates the likelihood of a model, i.e., the probability density of the dwell-time sequence given the scheme. The parameters in the model are then chosen so as to maximize the likelihood values. The likelihood function was corrected for the effect of missed events using a first-order approximation assuming the total durations of missed events were negligible as compared to the total dwell-time durations (Roux and Sauve, 1985). Search of the likelihood surface was performed using a variable metric (quasi-Newton) method (Press et al., 1992), where the partial derivatives of the likelihood function were calculated analytically for rapid optimization and the second-order inverse Hessian matrix was progressively built upon the information accumulated from successive line minimizations. Iterations of the algorithm were terminated when all gradients were sufficiently small, to ensure proper convergence. Precautions were always taken for possible local maximums by starting the algorithm with different initial values of rate constants. For visual inspection of the goodness of each fit, the probability density functions of open and closed components were evaluated from the fitted model parameters and superimposed on the experimental dwell-time histograms for direct comparisons (Fig. 3 *B*).

RESULTS

We describe here some general properties of the gating of VR1 including burst characteristics, dwell-time distributions, and correlations between closed and open components. The results were based on five to 16 excised membrane patches, as indicated. Each patch contained results from three to six different concentrations spanning 0.1–10 μM, and each concentration was recorded for 0.5–2 min. This typically resulted in a few hundred opening and closing events at low concentration to several thousands at high concentrations.

Single-channel activity

VR1 is activated by capsaicin at submicromolar concentrations. Fig. 1 illustrates representative single-channel recordings from a patch perfused with different levels of capsaicin. At low to medium concentrations, the activity comprised long closures, typically in the order of hundreds of ms. Such long closures were absent at high capsaicin concentrations, leading to an increase in the overall P_o.

The single-channel response to capsaicin was comparable to the results from whole-cell measurements (Caterina et al., 1997). The unitary current outwardly rectified with a conductance of 90 $\pm$ 3 pS at positive voltages (Fig. 1 *C*). While strongly voltage-dependent, the current amplitude was not affected by capsaicin (not shown). Subconductance levels were occasionally observed and were only slightly different from the main conductance (not shown). The dose-response curve suggests that ligand binding occurs with an apparent $K_d = 0.59 \pm 0.10$ μM and a Hill coefficient of $n_H = 1.5 \pm 0.4$ (Fig. 1 *B*). Single-channel measurements also revealed that the channel has an intrinsically low maximal P_o. The activity saturated at a concentration $\sim$3 μM with $P_o = 0.81 \pm 0.04$, which is significantly less than one. This limited attainable P_o was primarily due to the substantial population of brief closures that occurred throughout all capsaicin concentrations, as illustrated in Fig. 1 *A*.

The dose response illustrated in Fig. 1 was averaged from 16 experiments. The responses showed variations across experiments. The K_d was most consistent for all experiments and almost identical to the average, except two patches with $K_d \sim 0.3$ μM. The Hill coefficient was least stable, ranging typically from 1 to 4. The maximal activity also varied, with two occasions observed above 0.90. A close examination of the single-channel data suggests that the variations arose largely from the long closures between bursts. This is expected since the occurrences of such closures are relatively infrequent given the limited recording time. To avoid the complications caused by the variations, we drew our comparisons across concentrations only within patches.

Burst properties

The activity evoked by low to medium concentrations of capsaicin appeared as bursts of openings separated by long closures, or interburst ''gaps'' (Fig. 1 *A*). These gaps did not arise from the desensitization of VR1, since it requires cell integrity and external Ca^{2+}, both of which were deliberately avoided in our experiments (Caterina et al., 1997). Furthermore, the dose-response curve tended to increase monotonically with concentration, providing no indication that the gaps were due to open channel block by the agonist. Instead, these observations suggest that the occurrence of the interburst gaps is related to the intrinsic gating of the channel itself.

Fig. 2, *A* and *B* show the mean durations of the detected gaps and bursts as functions of capsaicin concentration. The results were averaged across experiments because few of these events were identified at any capsaicin concentration in a single experiment. Both bursts and gaps exhibited strong ligand dependence. The gaps were shortened with increasing capsaicin, while the bursts became elongated. At saturated

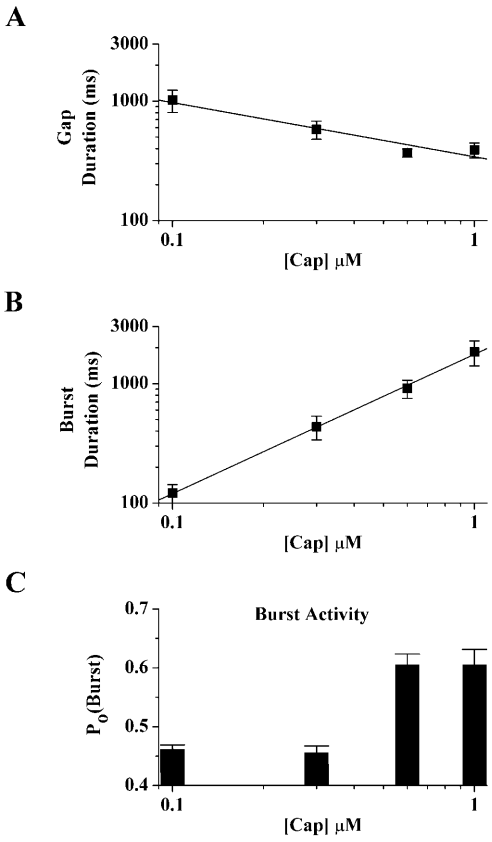

FIGURE 2 Concentration dependence of gaps and bursts. Gap (*A*) and burst (*B*) durations are plotted against capsaicin concentration and fit with an apparent linear function on a log-log scale. From the fits, gap duration decreases with concentration to the 0.45 ± 0.08 power, and burst duration increases to the 1.17 ± 0.03 power. Data is averaged over 14 experiments. (*C*) The open probability within the detected bursts increases with capsaicin, with an initial $P_o > 0.4$.

conditions, the gaps virtually vanished, suggesting that their occurrences are associated with ligand binding. The reduction of the gap durations follows a linear regression on a log-log plot with a slope ~0.45. This is lower than expected from a linear dependence of association rates on ligand concentrations, which suggests that these long closures may represent the concatenated durations of multiple capsaicin-bound states.

The dependence of burst length on capsaicin is intriguing. If ligand binding were complete before channel opening, the burst durations would be determined only by the dissociation rate from the fully-liganded closed state, which is independent of capsaicin. Since the burst length of the VR1 activity appeared to increase significantly with ligand concentration (Fig. 2 *B*), it strongly argues that open channel activity must have occurred before full binding of capsaicin. In the other words, even a partially-bound channel is capable of opening.

In addition to the burst length, the intraburst characteristics appeared to be concentration-dependent. For example, as shown in Fig. 2 *C*, the open probability within a burst increased with capsaicin concentration. This suggests that different levels of ligand binding may result in different types of bursts. A careful examination of the data shows that at least three types of burst activities can be distinguished (Fig. 1 *A*). At low capsaicin, bursts were mostly composed of brief openings with short to intermediate closures (≤100 ms); as the concentration was increased, the brief openings (<2 ms) were replaced with longer ones (~5 ms). At saturating capsaicin levels, two types of bursts became predominant. The first group comprised openings of intermediate duration (~5 ms) separated by brief closures (<2 ms); the second group, long openings (~15 ms), also interspaced by brief closures. Other, less frequent activities were also observed, adding to the complexity. Additionally, the relative population of long openings tended to increase with concentration, suggesting that more ligand binding also favors long openings.

Dwell-time distributions

The identification of multiple types of burst activity and possible activation of the channel from both partial and full capsaicin binding underlines the complexity of the gating mechanism of VR1. From single-channel data it is evident that there exist multiple types of openings and closures with different lifetimes. For example, brief closures appeared as flickers during periods of long openings in a burst, which were apparently different from the long ones that separate the bursts. To further quantify this complexity and characterize the gating, we examined the dwell-time distributions at different capsaicin concentrations.

Fig. 3 illustrates an idealized dwell-time sequence and the resultant dwell-time histograms. As expected, both closed and open histograms show multiple peaks, indicative of the presence of multiple states (Fig. 3 *B*). A fit of the histograms revealed at least five exponentials for the closed and three for the open class. Occasionally, an additional, infrequent, long open component was required to best fit the histogram. Likewise, an extra closed component was necessary for some experiments particularly at low concentrations. Adding more components sometimes increased the likelihood slightly, but often did not improve the fit visually. Therefore, five closed and three open states appear to be a minimal estimate of the number of conformations involved in VR1 gating. Fig. 3 *C* shows the actual dwell-time durations along the record time. All the components appeared throughout the experiment, though some of them were relatively rare at certain extreme conditions. Therefore, their presence is not likely due to gating mode shifts or other stochastic fluctuations, but instead intrinsic to the capsaicin-dependent gating of the channel.

The closed time constants spanned over a wide range, from ~0.2 ms to 2 s, and not all conditions revealed the same number of components (Table 1). Generally, at higher

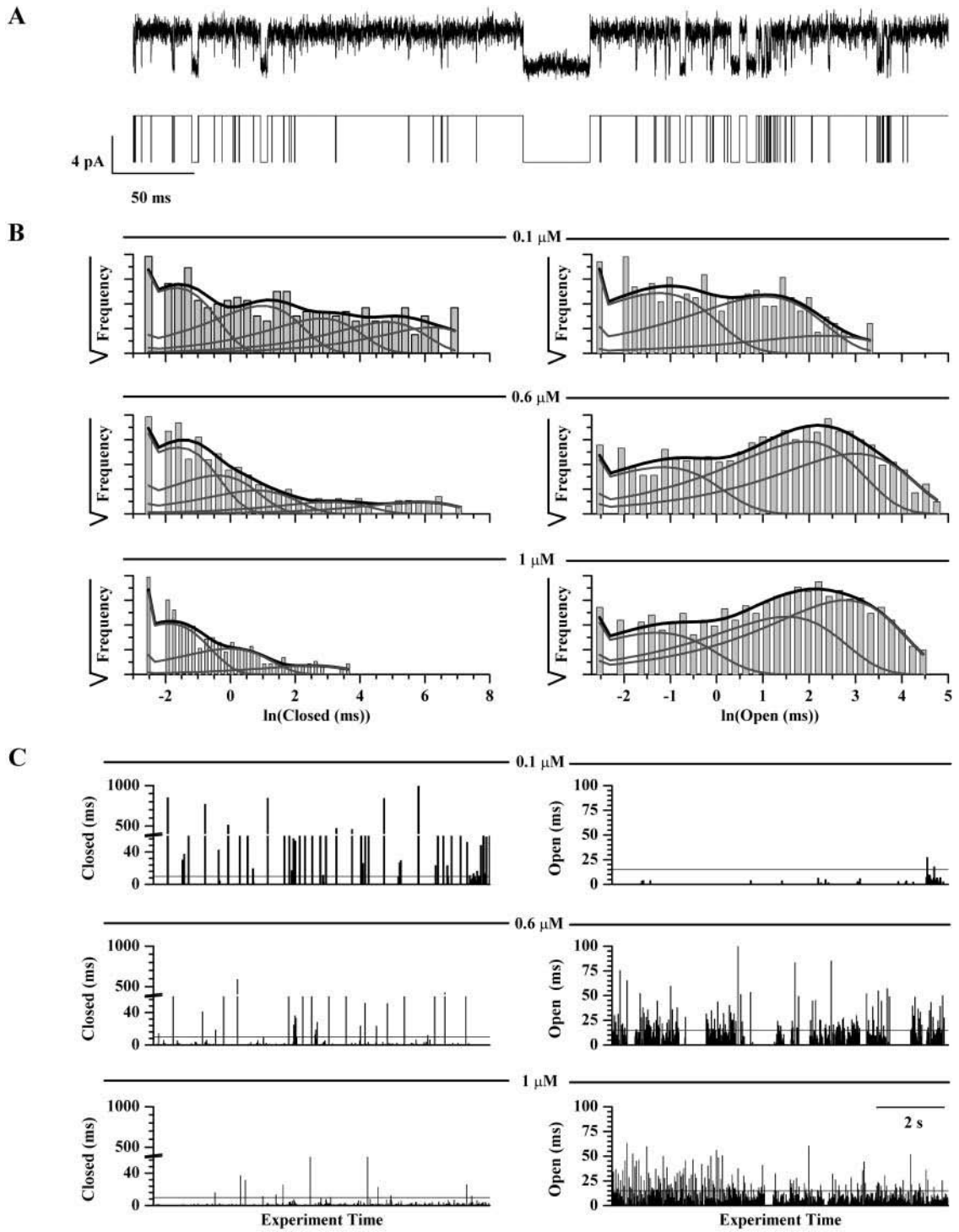

FIGURE 3 Idealization and dwell-time distributions. (*A*) Data were low-pass filtered at 10 kHz for idealization by the SKM method. The trace shown was filtered at 1 kHz. (*B*) Idealized data was used to construct closed and open dwell-time histograms with a dead time of 40 μs. The histograms for this experiment reveal as many as five closed and three open exponential components. At low capsaicin, all components are measurably populated. Increasing concentration favors the short closed and long open components. The fits are shown superimposed on the histograms as are the individual component distributions. For ease of visualization, the histograms are plotted after the Sigworth-Sine transformation (i.e., $\sqrt{\text{frequency}}$ versus ln(duration)). (*C*) The durations of the events are plotted against experiment time, showing the temporal distribution of all components at each concentration. With increasing concentration, long closures become fewer and long openings more abundant, consistent with the dwell-time histograms. Horizontal lines indicate the longest concentration-independent closed (10 ms) or open (15 ms) dwell times in the respective plots.

TABLE 1 Time constants from a single experiment at multiple capsaicin concentrations

[Cap] μM	Closed (ms)					Open (ms)		
0.1	0.16	2.3	14	108	435	0.26	2.6	9.4
0.3	0.17	1.3	8.1	194	2322	0.28	3.4	28
0.6	0.17	0.59	2.0	19	305	0.28	6.0	18
1	0.13	0.90	11			0.25	4.1	15
3	0.16	0.71	1.7	12	180	0.24	4.2	15
10	0.14	0.59	4.3	152		0.3	2.5	7.2

Time constants determined from a fit of the duration histograms for the experiment in Fig. 3. The time constants are listed in order of duration; the actual correspondences across concentration are ambiguous since some of the components, particularly the long closed ones, are not present at all concentrations.

concentrations as few as three components were necessary. Fig. 4 illustrates the time constants and proportions of individual components at variable conditions. Capsaicin had the most profound effect on the two longest closed components, where both time constants and proportions decreased with concentration, suggesting that they are directly involved in ligand binding. At low concentrations, they appeared to be the major contributors of the gaps. The three shortest components, on the other hand, were relatively more abundant at all concentrations. Their time constants varied relatively little with changes in capsaicin concentration, indicating that they are not directly associated with ligand binding. Instead, they are more likely to occur after binding, presumably corresponding to the closures inside bursts. The proportion of the shortest closed component increased with applied capsaicin, suggesting that ligand binding favors this flickery closure.

Occasionally, there was a certain ambiguity in determining the correspondences of the closed components across concentrations because not all of them appeared at all conditions. To minimize misclassification, we adopted the strategy of grouping the shortest ones first, since they were present at all conditions, and the remainder with the long ones. As a result, the impact of misclassification, if any, was most likely on the assignment of the intermediate closed component, which indeed shows a greater variance than the others across experiments. It is possible that there is actually more than one component represented here. The concentration dependence of the time constant and proportion of this aggregate was similar to the longer closed components, highlighting the possibility of more capsaicin-dependent closures.

In contrast to the closed components, all the open ones were well populated at all concentrations (Fig. 4 *C*). Their proportions were substantial, with the lowest $>10\%$, making it relatively easy to determine the correspondence between different components from different conditions. The frequency of long openings appeared to increase with applied capsaicin and the two short ones appeared to decrease, consistent with our observations from the burst activity variations. However, the short openings did not simply vanish at high capsaicin. Instead, they remained a significant portion even at saturated conditions, suggesting that the short openings are not exclusively from partially-bound channels.

Conceivably, ligand association may occur when the channel is open. This hypothesis, however, appears unlikely. While the proportions of individual open components varied with concentration, the time constants were remarkably stable, as shown in Fig. 4. They were either not significantly dependent on capsaicin or only weakly so, suggesting that capsaicin association is unlikely to occur when the channel is open (Fig. 4 *B*).

Dwell-time correlations

The one-dimensional dwell-time distributions lack the second-order information about correlations between closed and open components, which is essential in understanding transitions between states. To explore the existence of such correlations, we extended our analysis to two-dimensional distributions. Fig. 5 *A* shows the mean open times adjacent to, both before and after, closed dwell-times of specific durations. From the figure, we see that the longer the duration of the closed interval, the briefer the mean duration of the adjacent openings. This is in good agreement with our previous observation from the burst analysis that long openings tend to occur immediately before and after brief closures and that brief openings tend to precede or follow long closures. Moreover, the plots for the openings before and after closures overlap at all concentrations, implying that the system was microscopically reversible and that the gating of the channel was in thermodynamic equilibrium (Kerry et al., 1988; McManus and Magleby, 1989).

Fig. 5 *B* shows in more detail the coupling of openings to specific closed dwell-times, with durations divided into three ranges, long (>7 ms), intermediate (0.7–6 ms), and short (<0.7 ms). These three distributions have generally distinct appearances; for example, a significant population of brief openings is found adjacent to long closures but not to short ones. Such differences suggest that the gating of the channel must involve multiple opening pathways, otherwise there would be no correlation between open and closed dwell-times, and the two-dimensional distributions in the figure should be identical and the same as the one-dimensional distributions. Further examination of these distributions shows that the openings adjacent to short closures exhibit a peak at long durations and the openings adjacent to long closures exhibit a peak at short durations, suggesting that the channel may open from either short or long closures, likely corresponding to low or high levels of ligand binding, respectively.

Besides the aforementioned dwell-time distributions, we also explored the complexity of the gating by taking into account the correlations between openings and closures. From the one-dimensional distributions, we were able to resolve a minimum of five closed and three open

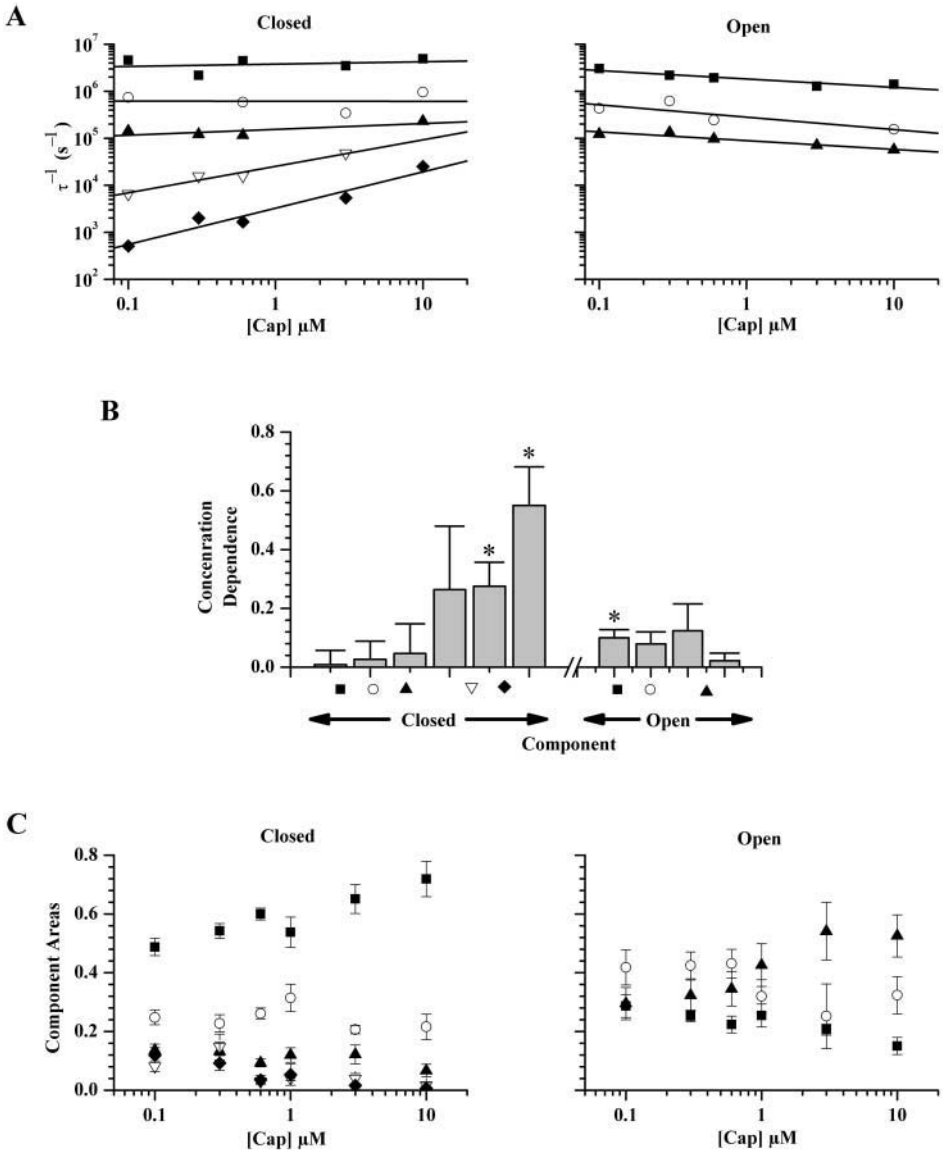

FIGURE 4 Effects of capsaicin on dwell-time components. (*A*) The reciprocals of the component time constants from the experiment in Fig. 3 are shown against capsaicin concentration. In this patch, up to five closed and three open components were sufficient to describe the dwell-time histograms. The concentration dependences were fit to the function $1/\tau = k \times [Cap]^{nH}$, where k is the binding rate constant and n_H is the cooperativity (in the simplest case, it is the number of ligand binding sites). The values of n_H were significantly greater than 0 for the two longest closed components (0.56 ± 0.08 and 0.77 ± 0.11). Assuming that these two involve only a single capsaicin binding, the corresponding concentration-dependent rate constants are 25.3 ± 0.8 and $3.3 \pm 0.5\ s{-}1\ \mu M^{-1}$. (*B*) Across 14 experiments, only the longest two closed components are significantly concentration-dependent, as indicated by an asterisk ($P < 0.05$), one open is weakly dependent ($n_H = 0.1$), and all others are insignificant. Correspondences between components were estimated based on the number and magnitude of the time constants. Unlike the patch in *A*, some histograms exhibited six closed and four open components. Therefore, for completeness, all six closed and four open components are shown here. (*C*) The proportions of the components were determined from the relative areas in the dwell-time histogram fits. Here, the population of short closures and long openings increase with concentration at the expense of the other components. Labeling across panels is identical with the longest three closed and two open components from *B* combined together in *C*.

components. Fitting of the full two-dimensional distributions showed that the gating of the channel is likely more complex, involving as many as seven closed and five open states. There were a total of four more components compared to the one-dimensional histograms, two for each class, which generally appeared to be short in duration. These additional components were undetected in the one-dimensional distributions, because of their similar time constants; however, the two-dimensional fits were able to resolve them separately by taking advantage of the distinct distributions of their adjacent components.

DISCUSSION

This study was intended to elucidate the gating mechanisms of VR1 through the determination of the kinetic characteristics of channel activity evoked by capsaicin. Dose-response curves, burst properties, dwell-time distributions, and correlations between closed and open dwell-times were investigated. Many aspects of the gating process, including the number of binding sites, the number of conformational states, different entry pathways to openings, and existence of multiple open conformations as well as the general complexity of the gating, were discussed. Our primary results are: 1), the channel has multiple binding sites with at least five to seven closed and three to five open conformations; 2), ligand association preferentially occurs to the closed conformations; 3), partial binding can lead to channel opening; and 4), higher levels of ligand binding favor longer openings. The results provide an important starting point in trying to understand the gating mechanism of VR1.

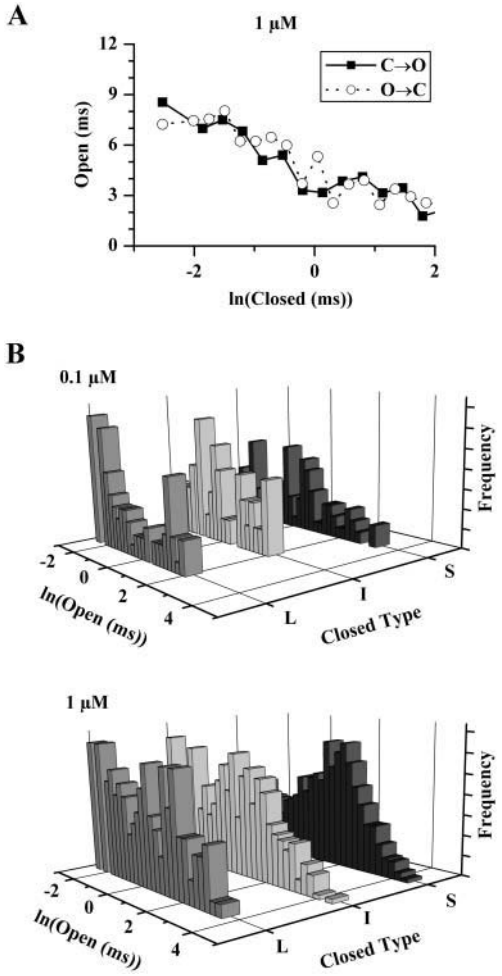

FIGURE 5 Coupling between open and closed events. (*A*) The average durations for openings adjacent to specific closures were determined for closed events up to 100 ms from the patch in Fig. 3. The duration of openings decreases with longer closures. Solid line represents openings after the closed events, and dotted line the openings preceding them. (*B*) Dwell-time histograms for openings adjacent to long (*L*, >7 ms), intermediate (*I*, 0.7–7 ms), or short (*S*, <0.7 ms) closures at low and high capsaicin. A significant peak is observed for short openings adjacent to long closures, which is not found adjacent to short closures. Furthermore, a substantial population of long openings adjacent to short closures is observed, particularly at high capsaicin. The areas were normalized to unity for comparison.

Multiple binding sites

In this study, the number of binding sites was estimated in two ways. The single-channel dose-response curve suggested at least two ligand binding sites, which is comparable to previous estimates from whole-cell measurements. Additionally, the dwell-time distributions revealed two closed components that are strongly dependent on capsaicin concentration, indicating that they are involved in ligand binding.

Although both approaches suggest two functional binding sites, this is likely an underestimate due to the limitations of these approaches. The dose-response curve is less sensitive to short closures than to long ones. It is possible that some binding steps are brief, so their occurrences are insignificant in contribution to the overall P_o as compared to other long closures. Also, the Hill coefficient is necessarily a lower limit. This value is equal to the number of ligand bindings only under the assumption that all bindings are completely cooperative, which is unrealistic. As a result, the total number of bindings is underestimated.

The estimate from the dwell-time distributions can be biased in several ways. First, among all the closed components, the two longest ones showed the strongest concentration dependences. However, these long closures were relatively infrequent compared to the short ones. As a result, they did not form clear peaks in the histograms. It is conceivable that they may actually represent an aggregation of multiple closed states that are also associated to direct bindings. Second, the intermediate closed component showed relatively large variations across experiments. In some experiments, it exhibited a statistically significant dependence on concentration, and in others it was only weakly dependent. This variation is likely due to the presence of more than the one component represented here, one of which may be involved in ligand binding. Therefore, the true number of capsaicin-dependent components may be underestimated.

Despite these limitations, it is evident that the channel has multiple functional binding sites. Chimeric studies between the capsaicin-insensitive chick VR1 and rat VR1 suggest that the TM2-3 linker of the polypeptide may be involved in capsaicin binding (Jordt and Julius, 2002). Furthermore, secondary structure analyses and biochemical studies suggest that VR1 belongs to the super-family of six transmembrane channels (Kuzhikandathil et al., 2001; Kedei et al., 2001; Rosenbaum et al., 2002). Channels in this family are formed by four monomers, suggesting that there may be as many as four ligand binding sites in the functional channel. Alternatively, it is also possible that the channel, even though a tetramer, may actually contain only two functional sites; for example, if they are formed at the interface of neighboring TM2–3 linkers. There is evidence suggesting that even under strong denaturing conditions the dimer form of VR1 remains intact (Rosenbaum et al., 2002). Although a dimer-to-dimer configuration would be consistent with our estimate, the exact number of ligand bindings still remains elusive.

Partial binding activity

Our observations strongly suggest that even the partially-bound channel is capable of inducing activity. This is supported by several lines of evidence. First, both burst length and intraburst characteristics were dependent on ligand concentration. Second, the one-dimensional open dwell-time distributions varied with capsaicin, though the time constants of the components were unchanged. Third, the two-dimensional dwell-time distributions revealed that

the openings adjacent to short, medium, and long closures have different distributions. These observations cannot be rationalized by models that lack openings from partially-liganded closed states.

The nature of the partially-liganded activities of VR is less certain. In some channels, different numbers of ligand bindings have been suggested to result in different conductance levels (Ildefonse and Bennett, 1991). VR1 also appeared to show subconductance levels; however, their occurrences were infrequent and did not appear correlated with the concentration of capsaicin or the kinetics of openings and closings. Therefore, it appears unlikely that the partially-liganded openings of VR1 are directly associated with the subconductances of the channel. Instead, it is more likely that the partially-liganded activities differ in their kinetics.

Our burst analysis indicated that there are at least three types of bursts, which differ in length, P_o, and open and closed durations. These features were highly correlated with ligand concentration, suggesting that the different types of burst activities may reflect different numbers of ligand molecules bound. If this is true, the number of variations in the bursts suggests at least three binding sites, which is within the range we had estimated from the dwell-time fits.

Multiple opens

From the analysis of dwell-time distributions it is evident that the gating of VR1 is likely complicated and involves multiple open states. The one-dimensional histograms revealed at least three to four kinetically different open conformations, but the actual number may be even higher as suggested by the two-dimensional distributions. Given the existence of multiple open states and that the channel exhibits partial binding activity, one question to ask is whether the different openings arise from a different number of ligand bindings separately, or can multiple open states be reached from each level of binding. Partially-liganded openings have been observed in other channels, and it is commonly assumed that each binding gives rise to a single type of opening, with partial binding leading to brief ones and full binding to long ones (Fig. 6 *A*).

Although our results provide no definitive answer, it appears that a scheme with a single type of opening from each level of binding would be too simple. Instead, each capsaicin binding, whether partial or full, tends to activate the channel with multiple types of openings. From the one-dimensional histograms, we observed that at low concentration brief to short openings were the dominant components. So, it appears that the openings induced by partial ligand binding tend to be brief in duration. But if the brief openings arose exclusively from partial binding, then we would expect them to vanish or at least to be significantly suppressed at high capsaicin. This does not seem to be the case, as the brief and short openings remained a large population even at saturated capsaicin concentrations. Furthermore, if the channel enters the singly-liganded or unliganded closed state, one would expect relatively long gaps to occur since the initial binding rate of capsaicin is slow. Again, we rarely observed such long closures at high concentrations.

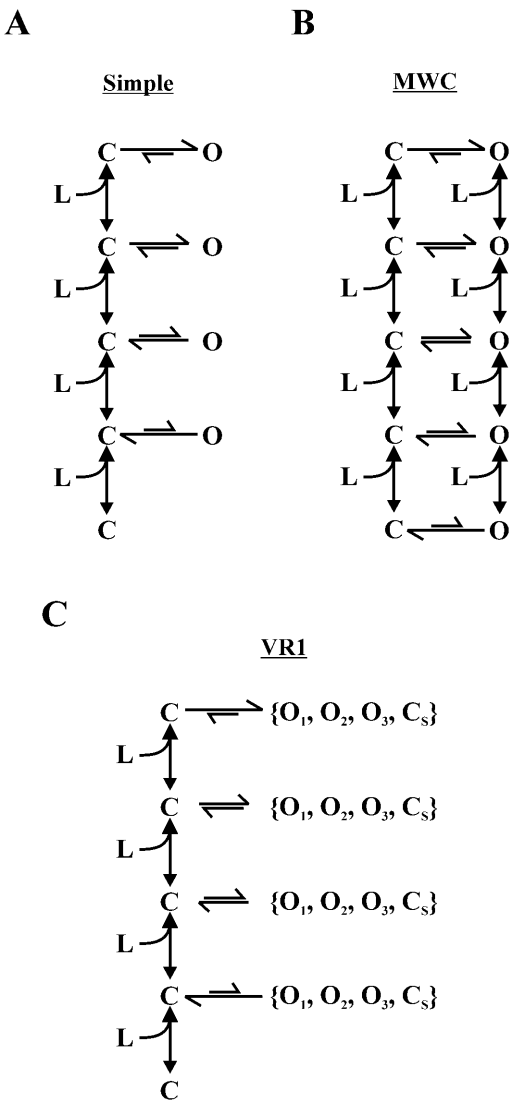

FIGURE 6 Models with partially bound openings. (*A*) In the simple branch model, the shortest open state is reached by a single ligand binding. At saturated concentration, the channel is fully bound, leading exclusively to the longest open state. (*B*) The MWC model describes the allosteric effect of ligand binding leading to channel opening. Similar to the simple branch model, additional bindings favor longer openings; but unlike the simple branch model, binding can also occur with the open channel. (*C*) The proposed model for VR1 is a modification of the simple branch model. Instead of a single opening, each level of capsaicin binding can lead to multiple openings. Furthermore, a short closed state (*C*s) in each branch is added to reflect the closures within the bursts (there may be as many as three such short closed states associated with each branch, but only one is shown for simplicity). The exact configuration of the branches is uncertain.

Another line of argument in support of this view comes from the closed dwell-time distributions. There was a significant amount of short closures existing ubiquitously over a wide range of capsaicin concentrations, and even after satu-

ration they constituted at least three components. This is in contrast to the prediction that there would be only one population of closures left after saturation, provided that there is only a single open state from each level of ligand binding. Based on these observations, it appears more likely that the long openings occur along with the short ones. That is, the different types of open states are accessible from any number of ligand bindings. With more ligands bound, the longer open states tend to be favored. This would explain why long openings are more probable at, but not exclusive to, high capsaicin concentrations. Furthermore, these openings are likely to occur in conjunction with short closures of at least three different types. These closures are independent of capsaicin, they are highly accessible even in the fully liganded state, and their frequent occurrence is the major factor that limits the maximal attainable P_o of the channel.

Possible mechanisms

The results obtained in this article provide strong constraints on the possible mechanisms applicable to the gating of VR1 channels. One well-studied model is the Monod-Wyman-Changeux (MWC) allosteric scheme (Fig. 6 *B*), which has been applied to several ligand-gated channels including the acetylcholine, glutamate, and purine (P2X) receptors, and the chloride and calcium-activated potassium channels (Blatz and Magleby, 1986; McManus and Magleby, 1991; Cox et al., 1997; Changeux and Edelstein, 1998). In this model, the effect of ligand binding is to shift the closed-open equilibrium toward the ligand-bound, open states. One appealing feature of the model is its generality. Although conceptually simple, it is flexible and can accommodate numerous kinetically different open and closed states.

When applied to VR1, the MWC model needs to be modified in several aspects. First, the open time constants are weakly concentration-dependent, suggesting that ligand-dependent transitions between the open states in the model are unnecessary. This is a significant restriction, since with these transitions the model is cyclic, and cyclic models are intrinsically ambiguous to identify (Fredkin et al., 1985). Second, no openings are observed in the absence of capsaicin, suggesting that the unliganded open state is unnecessary. Third, our inference of the existence of partially-bound openings confirms the necessity of the branches, though the exact number of branches remains uncertain. Simple sequential models do not provide adequate complexity to give rise to the observed correlations between closed and open states. Finally, the analysis described above argues that the open branches are necessarily more complicated, likely consisting of multiple opens as well as closed states.

Based on these considerations, we suggest the model in Fig. 6 *C* as a possible scheme for the gating of VR1. The model captures all aspects of our observations. Similar to a proposed model of the NMDA receptor, bursts are generated by openings and short closures in the branches (Kleckner and Pallotta, 1995). The concentration-dependent burst lengths are controlled by the different rates leaving each branch. A single capsaicin binding can open the channel, but the bursts are short because the leaving rate is fast. At higher levels of binding, the equilibrium rate constant favors the occupancy of the top branch, thereby increasing burst length and, consequently, overall P_o. The variation in the proportions of openings results from the presence of multiple open states in each branch and the differences in their connectivity. Lastly, the capsaicin-independence of the open durations results from the lack of ligand-dependent transitions between them.

An intriguing feature suggested by the model is that the channel activity evoked by capsaicin is restricted. Capsaicin binding alone cannot achieve full P_o. There are secondary closed states that are tightly coupled to the openings on the branches. These closed states are independent of capsaicin, appear at all concentrations, and have a substantial occupancy, thereby restricting the maximal P_o. An open question is the nature of these closures. It is unknown whether they occur before the open states—in which case they represent another barrier besides capsaicin binding that the channel needs to traverse to open—or after the open states, which would suggest some desensitization mechanism. It is also interesting to know whether these closures are controlled by some extrinsic factor that was invariant in our experiments. To this extent, protons and temperature would be potential candidates, given that each of them alone can activate the channel. It is conceivable that the opening of the channel requires a combination of capsaicin, protons, and heat since the latter two are ubiquitously present.

It should be emphasized that the model is merely a working hypothesis. Many aspects of the model, such as the number of binding steps, the cooperativity of successive bindings, and the exact nature of the branches, remain elusive. An emerging picture from our analyses is the complexity of the gating of VR1. The channel not only has a large number of open and closed conformations, but also multiple opening pathways. This complexity may reflect the polymodal activation and modulation of the receptor. Both physical and chemical stimuli can activate the channel directly. For capsaicin alone, the gating can be modulated by many factors, including pH, voltage, phosphorylation, and oxidation of the channel (Caterina et al., 1997; Tominaga et al., 1998; Hayes et al., 2000; Piper et al., 1999; Premkumar and Ahern, 2000; Vyklicky et al., 2002). We chose to work at pH 7.4, 20–25°C, and +60 mV: recordings at other conditions are very different. This imposes a great challenge in future studies of the functional mechanisms of the channel: how does each individual effector modulate the channel and how do they interact?

We thank Drs. H. Strauss and A. Auerbach for assistance on oocytes.

This study was supported by grants R01-RR11114 and R01-GM65994 from the National Institutes of Health.

REFERENCES

Blatz, A. L., and K. L. Magleby. 1986. Quantitative description of three modes of activity of fast chloride channels from rat skeletal muscle. *J. Physiol.* 378:141–174.

Caterina, M. J., and D. Julius. 2001. The vanilloid receptor: a molecular gateway to the pain pathway. *Annu. Rev. Neurosci.* 24:487–517.

Caterina, M. J., M. A. Schumacher, M. Tominaga, T. A. Rosen, J. D. Levine, and D. Julius. 1997. The capsaicin receptor: a heat-activated ion channel in the pain pathway. *Nature*. 389:816–824.

Changeux, J. P., and S. J. Edelstein. 1998. Allosteric receptors after 30 years. *Neuron*. 21:959–980.

Clapham, D. E., L. W. Runnels, and C. Strubing. 2001. The TRP ion channel family. *Nat. Rev. Neurosci.* 2:387–396.

Colquhoun, D., and A. G. Hawkes. 1982. On the stochastic properties of bursts of single ion channel openings and of clusters of bursts. *Philos. Trans. R. Soc. Lond. B Biol. Sci*. 300:1–59.

Cox, D. H., J. Cui, and R. W. Aldrich. 1997. Allosteric gating of a large conductance Ca-activated K+ channel. *J. Gen. Physiol.* 110:257–281.

Forney, G. D. 1973. The Viterbi algorithm. *Proc. IEEE*. 61:268–278.

Fredkin, D. R., M. Montal, and J. A. Rice. 1985. Identification of aggregated Markovian models: application to the nicotinic acetylcholine receptor. Proceedings of the Berkeley Conference in Honor of Jerzy Neymann and Jack Kiefer. L. M. LeCam, and R. A. Olshen, editors. Wadsworth. pp. 269–289.

Garcia-Martinez, C., C. Morenilla-Palao, R. Planells-Cases, J. M. Merino, and A. Ferrer-Montiel. 2000. Identification of an aspartic residue in the P-loop of the vanilloid receptor that modulates pore properties. *J. Biol. Chem.* 275:32552–32558.

Hayes, P., H. J. Meadows, M. J. Gunthorpe, M. H. Harries, D. M. Duckworth, W. Cairns, D. C. Harrison, C. E. Clarke, K. Ellington, R. K. Prinjha, A. J. Barton, A. D. Medhurst, G. D. Smith, S. Topp, P. Murdock, G. J. Sanger, J. Terrett, O. Jenkins, C. D. Benham, A. D. Randall, I. S. Gloger, and J. B. Davis. 2000. Cloning and functional expression of a human orthologue of rat vanilloid receptor-1. *Pain*. 88:205–215.

Ildefonse, M., and N. Bennett. 1991. Single-channel study of the cGMP-dependent conductance of retinal rods from incorporation of native vesicles into planar lipid bilayers. *J. Membr. Biol.* 123:133–147.

Jordt, S. E., and D. Julius. 2002. Molecular basis for species-specific sensitivity to ''hot'' chili peppers. *Cell*. 108:421–430.

Jordt, S. E., M. Tominaga, and D. Julius. 2000. Acid potentiation of the capsaicin receptor determined by a key extracellular site. *Proc. Natl. Acad. Sci. USA*. 97:8134–8139.

Julius, D., and A. I. Basbaum. 2001. Molecular mechanisms of nociception. *Nature*. 413:203–210.

Jung, J., S. W. Hwang, J. Kwak, S. Y. Lee, C. J. Kang, W. B. Kim, D. Kim, and U. Oh. 1999. Capsaicin binds to the intracellular domain of the capsaicin-activated ion channel. *J. Neurosci.* 19:529–538.

Kedei, N., T. Szabo, J. D. Lile, J. J. Treanor, Z. Olah, M. J. Iadarola, and P. M. Blumberg. 2001. Analysis of the native quaternary structure of vanilloid receptor 1. *J. Biol. Chem.* 276:28613–28619.

Kerry, C. J. R. L., R. L. Ramsey, M. S. P. Sansom, and P. N. R. Usherwood. 1988. Glutamate receptor channel kinetics: the effect of glutamate concentration. *Biophys. J.* 53:39–52.

Kleckner, N. W., and B. S. Pallotta. 1995. Burst kinetics of single NMDA receptor currents in cell-attached patches from rat-brain cortical neurons in culture. *J. Physiol.* 486:411–426.

Kuzhikandathil, E. V., H. Wang, T. Szabo, N. Morozova, P. M. Blumberg, and G. S. Oxford. 2001. Functional analysis of capsaicin receptor (vanilloid receptor subtype 1) multimerization and agonist responsiveness using a dominant negative mutation. *J. Neurosci.* 21:8697–8706.

Magleby, K. L., and D. S. Weiss. 1990. Identifying kinetic gating mechanisms for ion channels by using two-dimensional distributions of simulated dwell times. *Proc. R. Soc. Lond. B Biol. Sci.* 241:220–228.

McManus, O. B., and K. L. Magleby. 1989. Kinetic time constants independent of previous single-channel activity suggest Markov gating for a large conductance Ca-activated K channel. *J. Gen. Physiol.* 94:1037–1070.

McManus, O. B., and K. L. Magleby. 1991. Accounting for the Ca^{2+}-dependent kinetics of single large-conductance Ca^{2+}-activated K+ channels in rat skeletal muscle. *J. Physiol.* 443:739–777.

Piper, A. S., J. C. Yeats, S. Bevan, and R. J. Docherty. 1999. A study of the voltage dependence of capsaicin-activated membrane currents in rat sensory neurones before and after acute desensitization. *J. Physiol.* 518:721–733.

Premkumar, L. S., and G. P. Ahern. 2000. Induction of vanilloid receptor channel activity by protein kinase C. *Nature*. 408:985–990.

Press, W. H., S. A. Teukolsky, W. T. Vetterling, and B. P. Flannery. 1992. Numerical Recipes in *C*. Cambridge University Press, Cambridge.

Qin, F., A. Auerbach, and F. Sachs. 1996. Estimating single channel kinetic parameters from idealized patch-clamp data containing missed events. *Biophys. J.* 70:264–280.

Qin, F., A. Auerbach, and F. Sachs. 1997. Maximum likelihood estimation of aggregated Markov processes. *Proc. R. Soc. Lond. B Biol. Sci.* 264:375–383.

Rabiner, L. R., J. G. Wilpon, and B. H. Juang. 1986. A segmental k-means training procedure for connected word recognition. *ATT Tech. ET J.* 65:21–31.

Rosenbaum, T., M. Awaya, and S. Gordon. 2002. Subunit modification and association in VR1 ion channels. *BMC Neurosci.* 3:4.

Rothberg, B. S., and K. L. Magleby. 1998. Kinetic structure of large-conductance Ca^{2+}-activated K+ channels suggests that the gating includes transitions through intermediate or secondary states—a mechanism for flickers. *J. Gen. Physiol.* 111:751–780.

Roux, B., and R. Sauve. 1985. A general solution to the time interval omission problem applied to single channel analysis. *Biophys. J.* 48: 149–158.

Szallasi, A., and P. M. Blumberg. 1999. Vanilloid (Capsaicin) receptors and mechanisms. *Pharmacol. Rev.* 51:159–212.

Tominaga, M., M. J. Caterina, A. B. Malmberg, T. A. Rosen, H. Gilbert, K. Skinner, B. E. Raumann, A. I. Basbaum, and D. Julius. 1998. The cloned capsaicin receptor integrates multiple pain-producing stimuli. *Neuron*. 21:531–543.

Vyklicky, L., A. Lyfenko, K. Susankova, J. Teisinger, and V. Vlachova. 2002. Reducing agent dithiothreitol facilitates activity of the capsaicin receptor VR-1. *Neuroscience*. 111:435–441.

Welch, J. M., S. A. Simon, and P. H. Reinhart. 2000. The activation mechanism of rat vanilloid receptor 1 by capsaicin involves the pore domain and differs from the activation by either acid or heat. *Proc. Natl. Acad. Sci. USA*. 97:13889–13894.